International Journal of Automotive Technology, Vol. 7, No. 7, pp. 769–776 (2006)

1229–9138/2006/031–02

SIMPLE AND EFFECTIVE METHOD TO PREDICT THE OCCUPANT DYNAMIC RESPONSE UNDER SUDDEN IMPULSE LOADS

A. M. ELMARAKBI*

Department of Mechanical and Industrial Engineering, University of Toronto, Toronto, Ontario, M5S 3G8, Canada

(Received 22 May 2006; Revised 18 October 2006)

ABSTRACT–A mathematical model is developed in this paper to define the interaction between the occupant and vehicle passenger compartment and to predict the occupant dynamic response during a sudden impulse load. Two different types of occupants are considered in this study, child and adult occupants. The occupants are considered as lumped masses connected to the child seat and vehicle's body masses by means of restraint systems. In addition, the occupant restraint characteristics of seat belt and airbag are represented by stiffness and damping elements. To obtain the dynamic response of the occupant, the equations of motion of the occupants during vehicle collisions are developed and analytically solved. The occupant's acceleration and relative displacement are used as injury criteria to interpret the results. It is demonstrated from the numerical simulations that the dynamic response and injury criteria are easily captured and analyzed. It is also shown that the mathematical models are flexible, useful in optimization studies and it can be used at initial design stage.

KEY WORDS : Crashworthiness, Occupant protection, Restraint sustem, Injury criteria, Numerical simulations

1. INTRODUCTION

Analysis of a vehicle in a frontal crash event, in general, consists of studies of vehicle and occupant responses. Basically, there are two stages in a vehicle frontal collision with obstacles, namely: the primary and the secondary collisions. The primary collision is the collision between the vehicle front-end structure and an obstacle (barrier, vehicle, etc.). During the primary collision, the impact force generated between an obstacle and the vehicle induces a sudden deceleration of the vehicle structure. The secondary collision occurs between the occupant and the restraint system and/or the vehicle interior when the occupant continues to move forward and strikes the vehicle interior or interacts with the restraint system. The occupant safety restraint systems, such as seatbelt and airbag, define the interaction between occupant body and vehicle structure, and, thus, control the severity of dynamic effects imparted on the occupant.

For the protection of vehicle occupants in crash, regulatory agencies specify vehicle crashworthiness requirements in terms of impact force and acceleration experienced by occupant body parts. These requirements are measured on anthropomorphic dummies in crash test, and by specifying equipment requirements for active and passive restraint systems. The limit of the resultant acceleration, expressed as a multiple of the acceleration of gravity (g) at the location of accelerometer mounted in the test dummy upper thorax, as specified in FMVSS (1999a, 1999b), must not be more than 60 g.

The vehicle crashworthiness depends on many factors including the occupant size and mass (Mills and Hobbs, 1984; Hyde, 1992). A smaller mass occupant (such as a child) is likely to experience much higher deceleration, compared to an adult, for the given characteristics of vehicle structures and restraint systems. The restraint system and vehicle structures, designed to deliver the specified target requirements, may not be beneficial for children. Their soft bone structures, weaker muscles, heavy heads and smaller bodies expose them to higher risk of injuries during a vehicle crash. It is recommended to place the children in the rear passenger seats of a car to eliminate the risks of secondary impacts with vehicle interior features, such as the dashboard, steering wheel and windshield as specified in CMVSS (1999). Also, specially designed child car seats are used to integrate the child body with the seat and seat belts. However, the seat belt restraint system, if designed for adult occupant protection, may expose the smaller mass occupants to harmful amplitude deceleration during a crash.

The work presented in this paper includes developing and analyzing a mathematical model for two types of occupants, adult and child, involved in full and offset vehicle-to-vehicle frontal collisions. The influence of

*Corresponding author. e-mail: ahmed.elmarakbi@utoronto.ca

various crash situations on the dynamic response of the occupants is demonstrated by numerical simulations.

2. DYNAMIC RESPONSE ANALYSIS OF THE VEHICLE

Lumped mass models have been used since early 1970s for the analysis and design of automotive structures for safety during crash (Kamal, 1970). In these models, the major undeformable structural components are represented by lumped masses and the major deformable structural components are modeled as nonlinear spring elements, typically represented with the force-deformation data gained from experiments. Lumped parameter simulation has been employed for dynamic simulations and occupant analysis (Bennette *et al.*, 1991).

To predict the behavior of a vehicle involved in a head-on collision with another vehicle, the mathematical model shown in Figure 1 is used to obtain the dynamic response of the both vehicles.

In this model, the stiffness elements shown as springs with stiffness coefficients k_{ij} are the plastic deformation parts representing the longitudinal members in the front-end structure. The masses of the vehicle body and the bumper assembly are represented by M_{pi} and m_b, respectively.

The equations of motion of vehicle-to-vehicle frontal collision, as shown in Figure 1, can be written as the following equations.

$$M_{p1}\ddot{x}_{p1} + F_{11}(\delta_{11}) + F_{12}(\delta_{12}) = 0 \tag{1}$$

$$M_{p2}\ddot{x}_{p2} + F_{21}(\delta_{12}) + F_{22}(\delta_{22}) = 0 \tag{2}$$

$$m_b\ddot{x} + F_{21}(\delta_{12}) + F_{22}(\delta_{22}) - F_{11}(\delta_{11}) - F_{12}(\delta_{12}) = 0 \tag{3}$$

$$I_b\ddot{\theta}_b + F_{12}(\delta_{12})\cdot l_1 - F_{11}(\delta_{11})\cdot l_2 + F_{22}(\delta_{22})\cdot l_4 - F_{21}(\delta_{21})\cdot l_3 = 0 \tag{4}$$

where $\ddot{x}$ and $\ddot{x}_{p1}$ are the translation decelerations of the bumper assembly and passenger compartment (vehicle body), respectively. $\ddot{\theta}_b$ and I_b are the rotational deceleration and mass moment of inertia of the bumper assembly, respectively. l_i are the lengths between the plastic springs and the point (C.G) of rotation of the vehicle's bumper in offset collision.

The deformation of the plastic springs are given by

$$\delta_{11} = x_1 - x_{11},\ \delta_{12} = x_1 - x_{12} \tag{5}$$

$$\delta_{22} = x_2 + x_{22},\ \delta_{21} = x_2 + x_{21} \tag{6}$$

The displacements of the spring ends are defined as follows:

$$x_{11} = x + l_2\cdot\tan\theta_b,\ x_{12} = x - l_1\cdot\tan\theta_b \tag{7}$$

$$x_{21} = x - l_3\cdot\tan\theta_b,\ x_{22} = x + l_4\cdot\tan\theta_b \tag{8}$$

The forces of the plastic springs $F_{ij}(\delta_{ij})$, as shown in Figure 2, are defined using piecewise nonlinear functions in the displacement domain as follows:

$$F_{ij} = f_{0ij} + k_{ij}\cdot\delta_{ij} - F_{0ij} \tag{9}$$

where

$$k_{ij} = (k_{ij})_1,\ F_{0ij} = 0 \qquad \delta_{ij} \le \delta_{ij}^* \tag{9a}$$

$$k_{ij} = (k_{ij})_2,\ F_{0ij} = ((k_{ij})_2 - (k_{ij})_1)\cdot\delta_{ij}^* \qquad \delta_{ij} > \delta_{ij}^* \tag{9b}$$

where i=1,2 (i=1 represents the vehicle 1, and i=1,2 represents the vehicle 2). j=1,2 (i=1 represents the right longitudinal member, and j=2 represents the left longitudinal member).

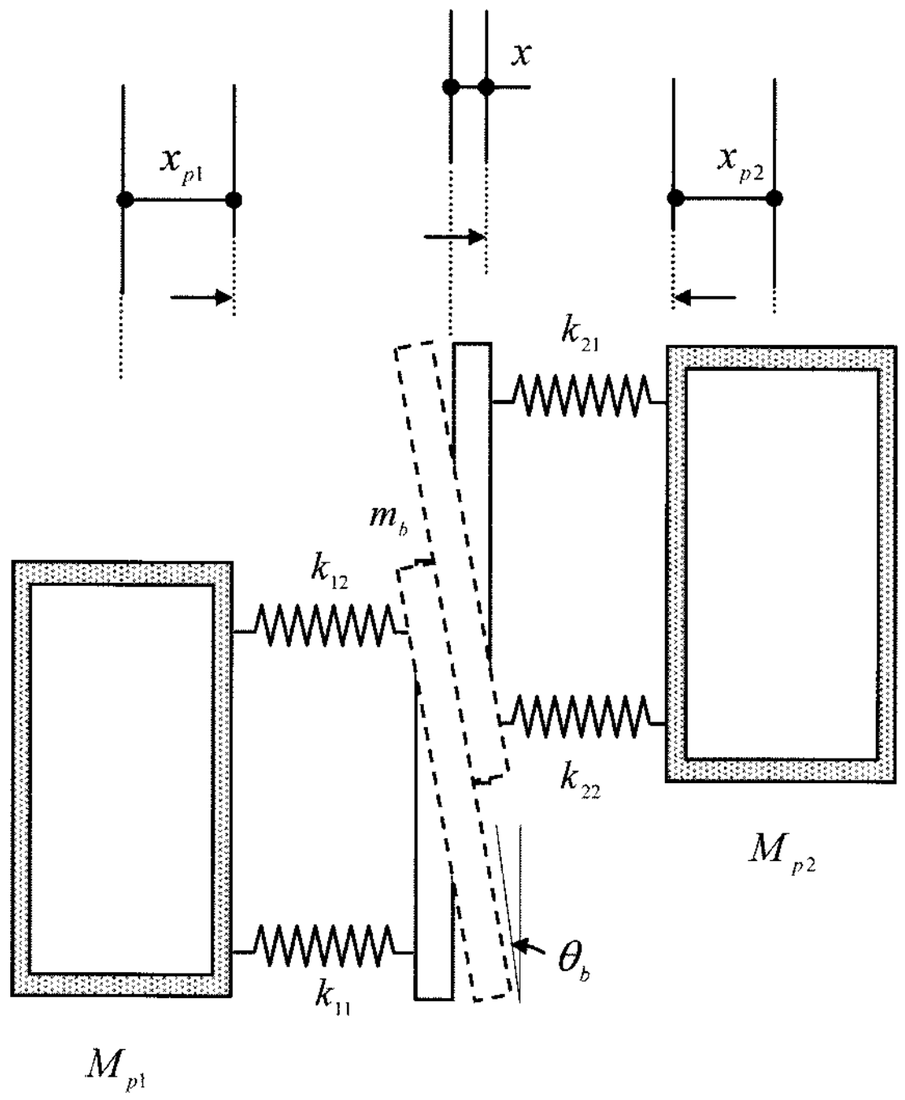

Figure 1. Vehicle-to-vehicle offset frontal collision.

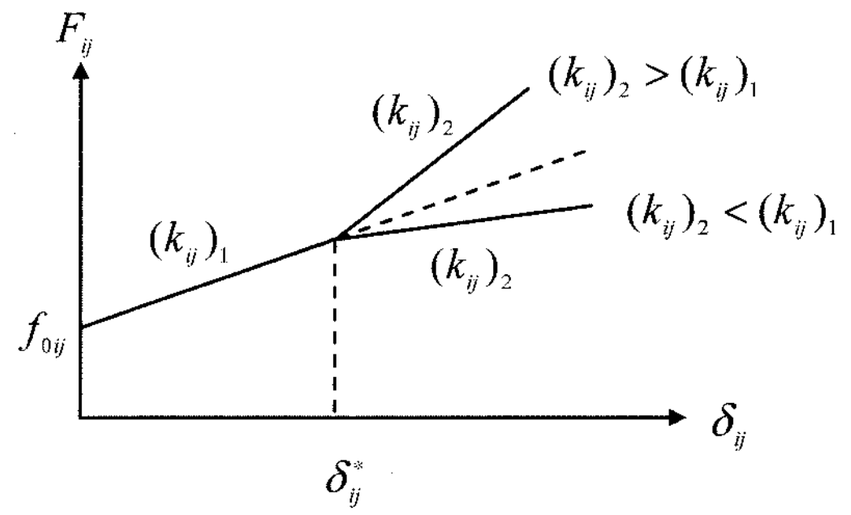

Figure 2. Force-deformation characteristics of the vehicle's longitudinal members.

3. DYNAMIC RESPONSE ANALYSIS OF THE OCCUPANT

The mathematical models shown in Figures 3 and 4 are used to define the interaction between the occupant and the vehicle body for both adult and child occupants, respectively. The occupant is considered as a lumped mass, connected to the vehicle's body mass by means of a restraint system. The occupant's restraint characteristics of seatbelt, airbag, and child seat are represented by stiffness k_i and damping coefficient c_i. Also, the mass of the occupant is represented by m_o. The subscripts a, c and s correspond to adult occupant, child occupant, and child seat, respectively.

To obtain the dynamic response of the occupant during the secondary impact, the equations of motion for the systems shown in Figures 3 and 4 can be derived as follows:

For adult occupant:

$$m_{aoi} \cdot \ddot{x}_{aoi} + f_{soi}(\delta_{aoi}) + f_{doi}(v_{aoi}) = 0 \tag{10}$$

and for child occupant:

$$m_{aoi} \cdot \ddot{x}_{aoi} + f_{soi}(\delta_{aoi}) + f_{doi}(v_{aoi}) = 0 \tag{11}$$

$$m_{si} \cdot \ddot{x}_{si} + f_{ssi}(\delta_{si}) + f_{dsi}(v_{si}) - f_{soi}(\delta_{coi}) - f_{doi}(v_{coi}) = 0 \tag{12}$$

where $\ddot{x}_{aoi}$, $\ddot{x}_{coi}$ and $\ddot{x}_{si}$ are the translation accelerations of the adult occupant, child occupant and child seat, respectively; $f_{soi}(\delta_{aoi})$, $f_{soi}(\delta_{coi})$, and $f_{ssi}(\delta_{si})$ are forces generated by plastic springs on the adult occupant, child occupant and child seat, respectively; $f_{doi}(v_{aoi})$, $f_{doi}(v_{coi})$ and $f_{dsi}(v_{si})$ are damping forces generated on the adult occupant, child occupant and child seat, respectively; δ_{aoi}, δ_{coi}, δ_{si}, v_{aoi}, v_{coi} and v_{si} are relative displacements and velocities of springs and dampers of the adult occupant, child occupant and child seat, respectively.

In case of crash analysis, the mass is always constant, while the damping and stiffness are not; they mainly depend on the velocity and displacement values. In this paper, the forces generated on the adult occupant by the spring $f_{aoi}(\delta_{aoi})$ as shown in Figure 5 can be defined as follows:

$$f_{aoi}\delta_{aoi} = k.\ (\delta_{aoi} - \delta^*_{aoi}) \tag{13}$$

where

$$k = 0 \qquad \delta_{aoi} \le \delta^*_{aoi} \tag{14}$$

$$k = k_{oi} \qquad \delta_{aoi} > \delta^*_{aoi} \tag{15}$$

Moreover, the damping force of the occupant is determined as

$$(f_{doi})(v_{aoi}) = c \cdot (v_{aoi} - v^*_{aoi}) \tag{16}$$

where

$$c = 0 \qquad v_{aoi} \le v^*_{aoi} \tag{17}$$

$$c = c_{oi} \qquad v_{aoi} > v^*_{aoi} \tag{18}$$

where δ^*_{aoi} is the initial slack length. The slack length represents the relative displacement of the adult occupant, δ_{aoi}, before the seatbelt becomes effective. The relative velocity of the occupant when the seatbelt becomes effective is defined by v^*_{aoi}. Similarly, forces generated on the child occupant by springs, $f_{soi}(\delta_{coi})$, and damping

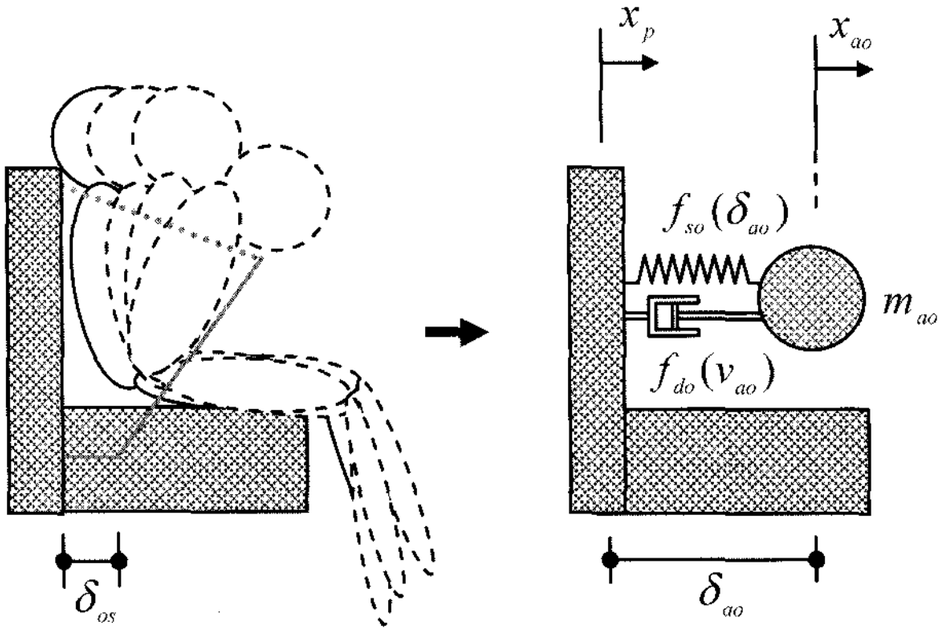

Figure 3. Mathematical model of the adult occupant in the secondary impact.

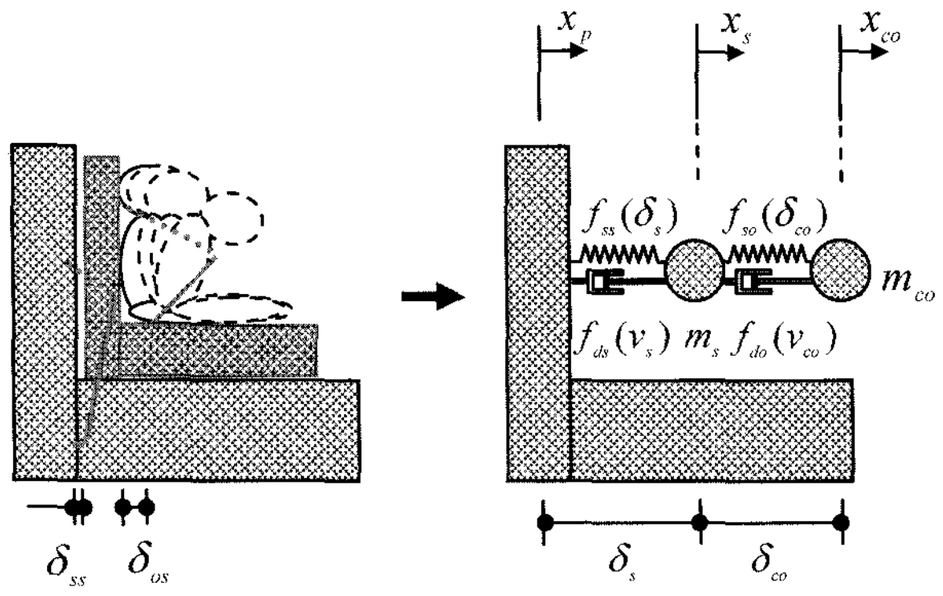

Figure 4. Mathematical model of the child occupant in the secondary impact.

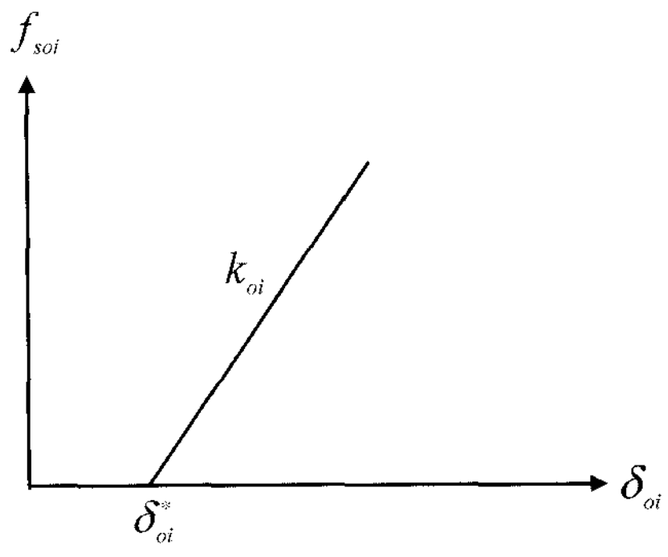

Figure 5. Force-deformation characteristic of the occupant.

forces, $f_{doi}(v_{coi})$, of the restraint system, as well as forces generated on the child occupant by the child seat, $f_{ssi}(\delta_{si})$ and $f_{dsi}(v_{si})$, respectively can also be defined as Equations (13)–(18).

The relative displacement of the spring, δ_{aoi}, and the velocity of the damper, v_{aoi}, of the adult occupant due to the restraint system are respectively defined as

$$\delta_{aoi} = x_{aoi} - x_{pi} \tag{19}$$

$$v_{aoi} = \dot{x}_{aoi} - \dot{x}_{pi} \tag{20}$$

Similarly, the relative displacements of the spring, δ_{coi}, and the velocity of the damper, v_{aoi}, of the child occupant due to the restraint system, as well as the relative displacements of the spring, δ_{ssi}, and the velocity of the damper, v_{ssi}, of the child seat are respectively defined as follows:

$$\delta_{coi} = x_{coi} - x_{si} \tag{21}$$

$$v_{coi} = \dot{x}_{coi} - \dot{x}_{si} \tag{22}$$

$$\delta_{soi} = x_{si} - x_{pi} \tag{23}$$

$$v_{ssi} = \dot{x}_{si} - \dot{x}_{pi} \tag{24}$$

Substituting Equations (13-20) into Equation (10) yields

$$m_{oi} \cdot \ddot{x}_{oi} + c \cdot \dot{x}_{aoi} + k \cdot x_{aoi} = f(t) \tag{25}$$

where

$$f(t) = f(t) = c(\dot{x}_{pi} + v^*_{aoi}) + k(x_{pi} + \delta^*_{aoi}) \tag{26}$$

The general solution of Equation (25) can be determined in the following

$$x_{oi} = e^{-\xi_{oi}\omega_{oi}t}(a\sin\omega_{doi}t + b\cos\omega_{doi}t) + \frac{1}{m_{oi}\omega_{doi}}\int_0^t f(\tau)e^{-\xi_{oi}\omega_{oi}(t-\tau)}\sin\omega_{doi}(t-\tau)d\tau \tag{27}$$

The occupant is subjected to the following initial conditions:

$$x_{aoi}(0) = 0, \dot{x}_{aoi}(0) = v_{oi} \tag{28}$$

Using the initial conditions of the occupant, Equation (27) can be rewritten as

$$x_{aoi} = e^{-\xi_{oi}\omega_{oi}t}\left(\frac{v_{oi}}{\omega_{doi}}\sin(\omega_{doi}t)\right) + \frac{e^{-\xi_{oi}\omega_{oi}t}\sin(\omega_{doi}t)}{m_{oi}\omega_{doi}}\int_0^t f(\tau)e^{\xi_{oi}\omega_{oi}\tau}\cos(\omega_{doi}\tau)d\tau - \frac{e^{-\xi_{oi}\omega_{oi}t}\cos(\omega_{doi}\tau)}{m_{oi}\omega_{doi}}\int_0^t f(\tau)e^{\xi_{oi}\omega_{oi}\tau}\sin(\omega_{doi}t)d\tau \tag{29}$$

where ξ_{oi} is the damping ratio $= c_{oi}/c_{coi}$, c_{coi} is the critical damping $= 2\omega_{oi}\omega_{oi}$, ω_{oi} is the nature frequency, and ω_{oi} is the damping frequency $= \sqrt{1-\xi_{oi}^2}$.

The velocity and the deceleration of the occupant can be obtained by differentiation of Equation (29). Similarly,

Equations (11)–(12) can be rewritten in the following form:

$$m_{coi} \cdot \ddot{x}_{coi} + c \cdot (\dot{x}_{coi} - \dot{x}_{si}) + k \cdot (x_{coi} - x_{si}) = f_1(t) \tag{30}$$

$$m_{oi} \cdot \ddot{x}_{oi} + c \cdot \dot{x}_{aoi} + k \cdot x_{aoi} = f(t)$$

$$m_{si} \cdot \ddot{x}_{si} + (c_s + c) \cdot \dot{x}_{si} + (k_s + k) \cdot x_{si} - c \cdot \dot{x}_{coi} - k \cdot x_{coi} = f_1(t) \tag{31}$$

where

$$f_1(t) = c \cdot v^*_{aoi} + k \cdot \delta^*_{coi} \tag{32}$$

$$f_2(t) = c_s \cdot (\dot{x}_{pi} + v^*_{si}) + k_s \cdot (x_{pi} + \delta^*_{si}) - f_1(t) \tag{33}$$

The values of displacement x_p and velocity $\dot{x}_p$ of the vehicle body, due to the sudden impact force generated between obstacle and vehicle, which induce a sudden deceleration of the vehicle structure, are determined by solving the set of equations in Sec. 2 (see Elmarakbi , 2004; Elmarakbi and Zu, 2004 and 2005, for further details). The functions $f(t)$ and $f_2(t)$ are depicted in Figures 6 and 7, respectively.

4. NUMERICAL SIMULATIONS

In this section, the analysis developed in the former section is verified by the presentation of the results for both mathematical models. The injury criteria are used to interpret the results. The main injury criteria of interest in this paper are the acceleration and the relative displacement of the occupant.

The following data are used in the numerical solution. The mass of adult and child occupants (m_{ao} and m_{co}) are taken as 80 and 18 kg, respectively. In addition, the mass of the child seat (m_s) is taken as 5 kg. The adult occupant's restraint characteristics of seatbelt and airbag are represented by stiffness k_{ao} of 98.1 kN/m with a slack distance δ^*_{ao} of 0.005 m and damping coefficient c_{ao} of 2.54 kN.s/m (50% of the critical damping). The restraint characteristics for the child occupant and child seat are

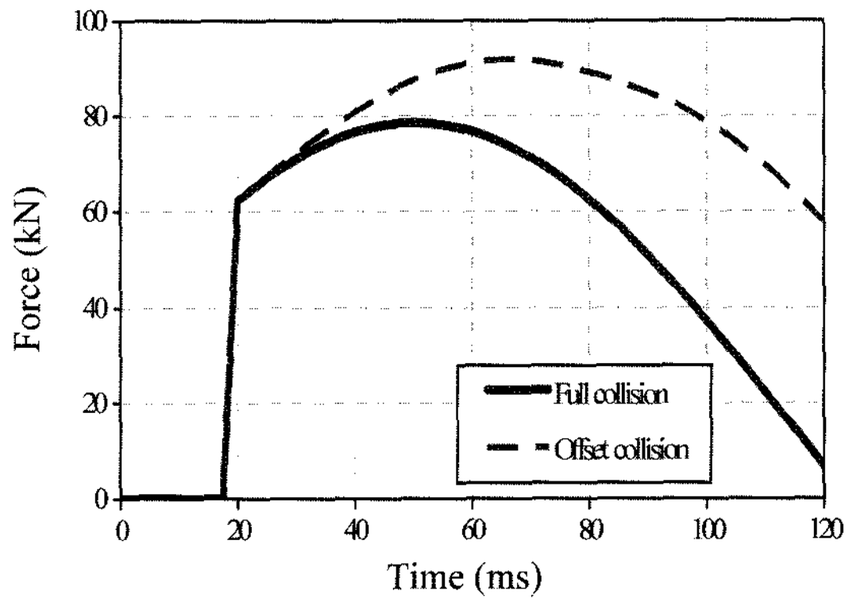

Figure 6. The impact force $f(t)$ in full and offset frontal collisions.

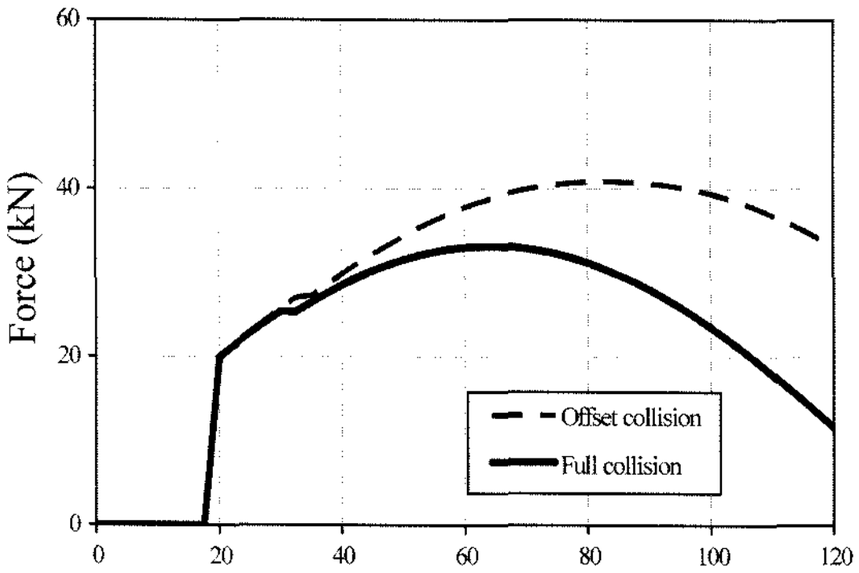

Figure 7. The impact force $f_2(t)$ in full and offset frontal collisions.

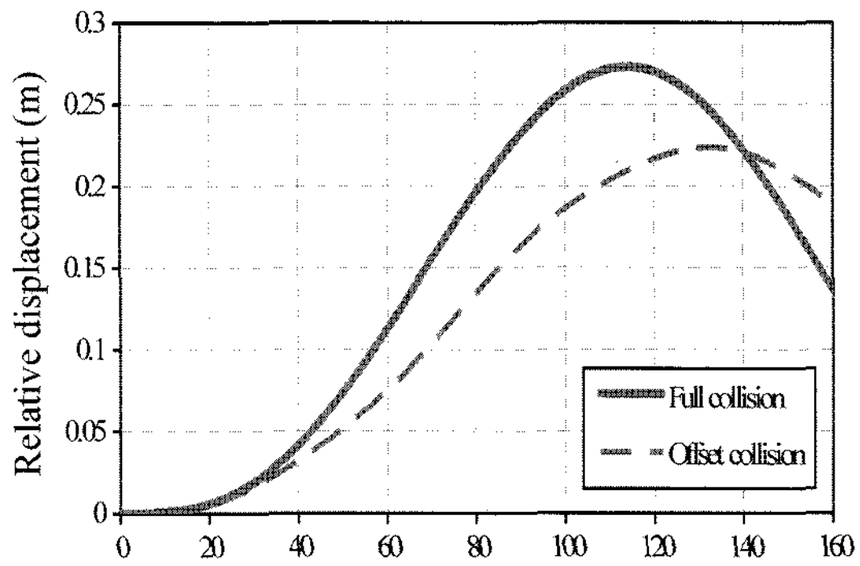

Figure 8. Relative displacement of the adult occupant in full and offset frontal collisions.

represented by stiffness k_{co} of 49 kN/m and k_s of 50 kN/m with a slack distance $\delta^*_{co} = \delta^*_s$ =0.005 m, respectively, and damping coefficients c_{ao} and c_s of 50% of the critical damping for both child occupant and child seat. The initial velocity of the vehicle and the occupant (v_o) is taken as 13.33 m/s.

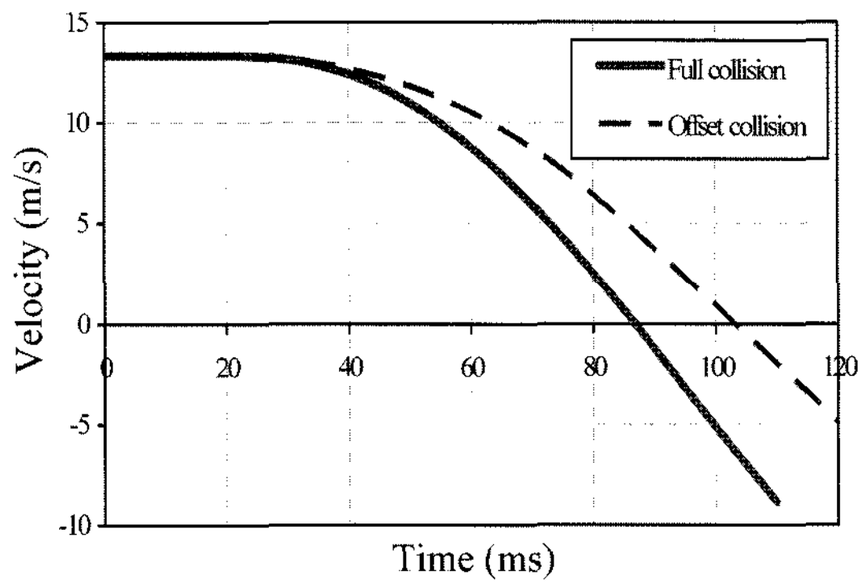

Figure 9. Velocity of the adult occupant in full and offset frontal collisions.

4.1. Adult Occupant

Two cases of simulation runs involving two vehicles in head-on collision are used. The first case involved a collision of two vehicles in a full frontal impact. The second case involved the two vehicles in an offset frontal collision.

The time histories of the relative displacement, velocity and acceleration of the occupant as obtained from the two simulations are shown in Figures 8, 9 and 10, respectively.

Figure 8 clearly shows the significant reduction in the occupant's relative displacement in the case of offset frontal collision. It can be noted that the occupant relatively displaced 0.22 m in the offset collision compared to 0.27 m in the full frontal collision. It is clear from Figure 9 that the occupant's velocity vanishes in a longer time zone in the offset collision than that in the full frontal collision. This indicates the time required to stop the vehicle in offset collision is larger than required in the full collision. The occupant's acceleration is depicted in Figure 10 for both cases. It is noticed that the occupant sustains more deceleration (40 g) in the full frontal collisions while in the offset collision, the occupants suffers lower acceleration (30 g).

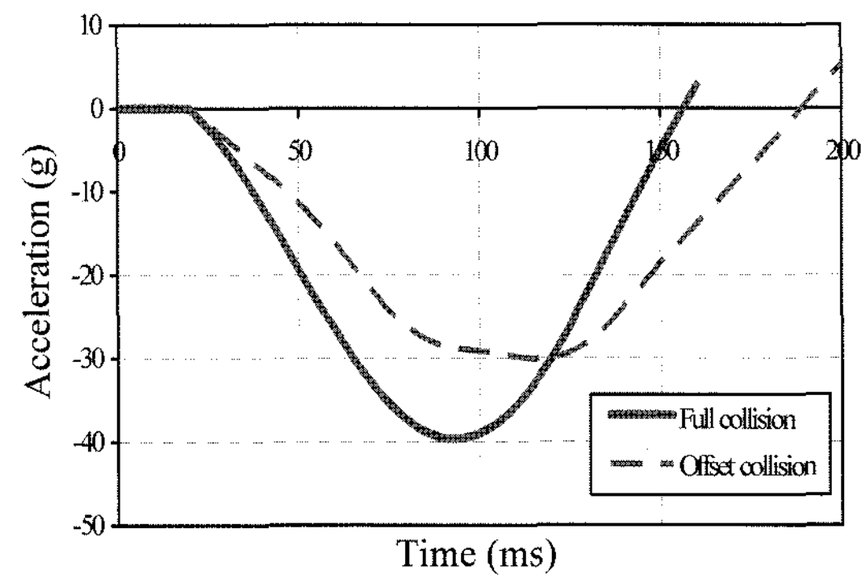

Figure 10. Acceleration of the adult occupant in full and offset frontal collisions.

The influence of the damping value as a percentage of the critical damping at a constant stiffness (98.1 kN/m) is discussed in the following Figures. Three different damping values of the occupant's restraint system, 10, 20, and 50% of the critical damping, are considered in this paper.

Figures 11, 12 and 13 show the relative displacement, velocity and acceleration of the adult occupant as obtained from the full frontal collision simulation. Figure 11 clearly shows a reduction in the displacement injury with increase in damping value. However, damping values have a slight influence on the velocity of the occupant as shown in Figure 12. Since the relative displacement decreases when increasing the damping values, the acceleration of the occupant decreases by increasing the damping values, as well as shown in

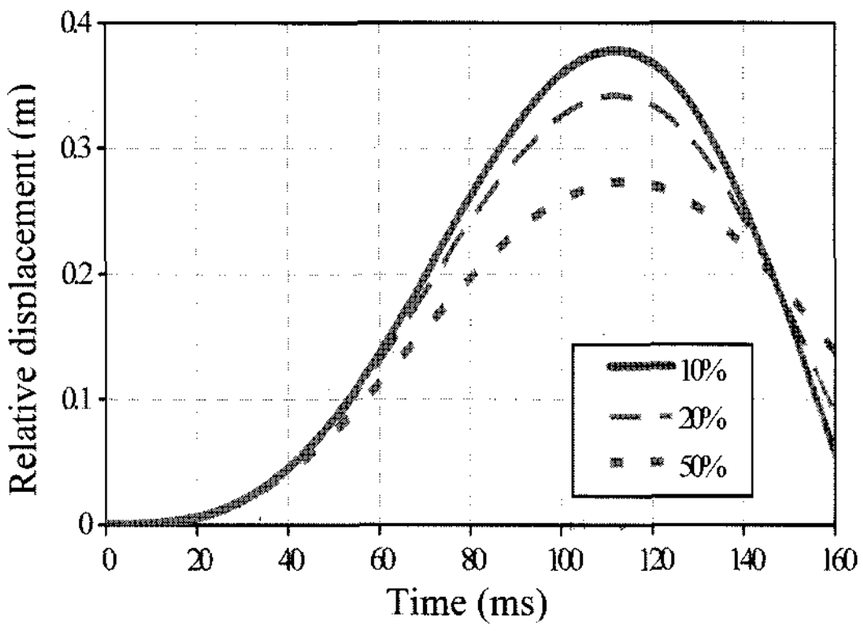

Figure 11. Relative displacement of the adult occupant in full frontal collision with different damping ratios.

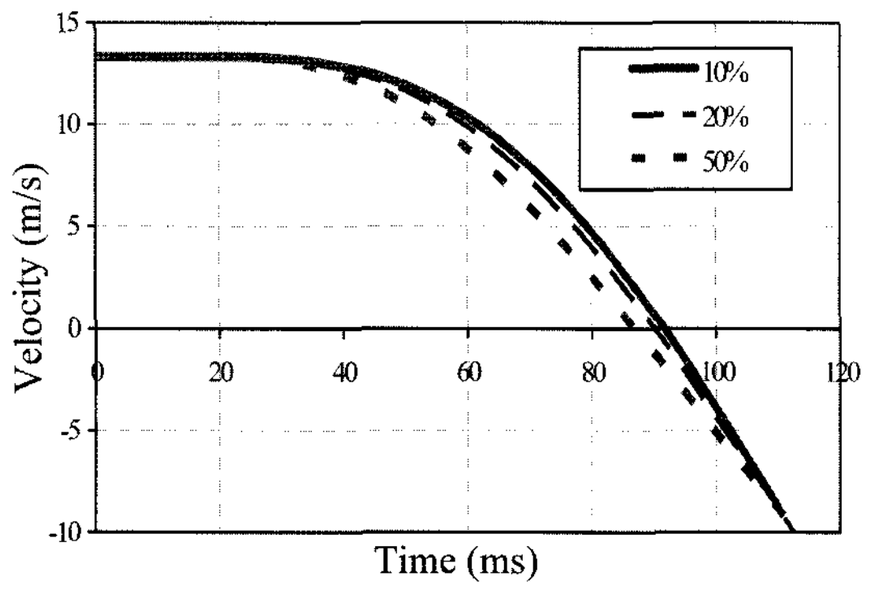

Figure 12. Velocity of the adult occupant in full frontal collision with different damping ratios.

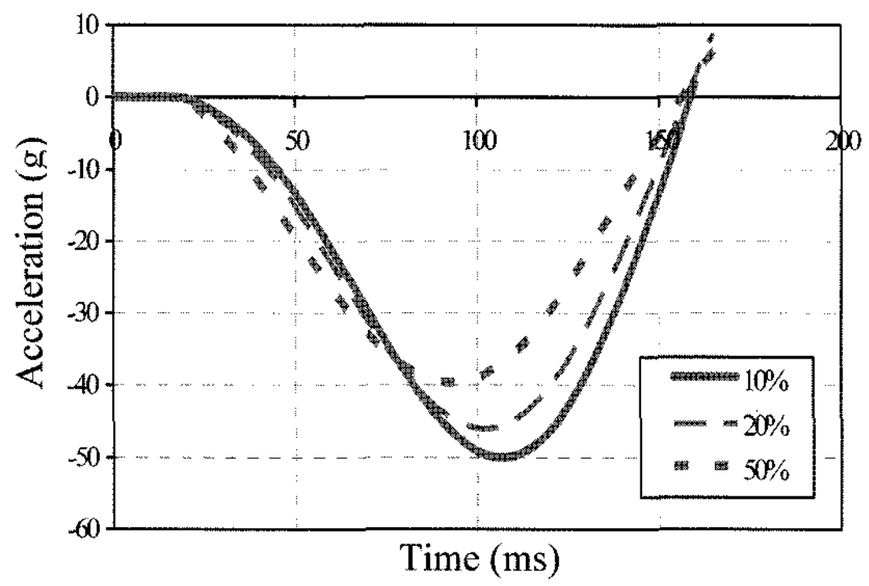

Figure 13. Acceleration of the adult occupant in full frontal collision with different damping ratios.

The influence of the stiffness value of the restraint system at a constant damping value of 50% of the critical damping is investigated. Three different stiffens values of the occupant's restraint system, 98.1, 39.24, and 19.62 kN/m, are considered in this paper. Figures 14, 15 and 16 show the relative displacement, velocity and acceleration of the adult occupant as obtained from the full frontal collision simulation.

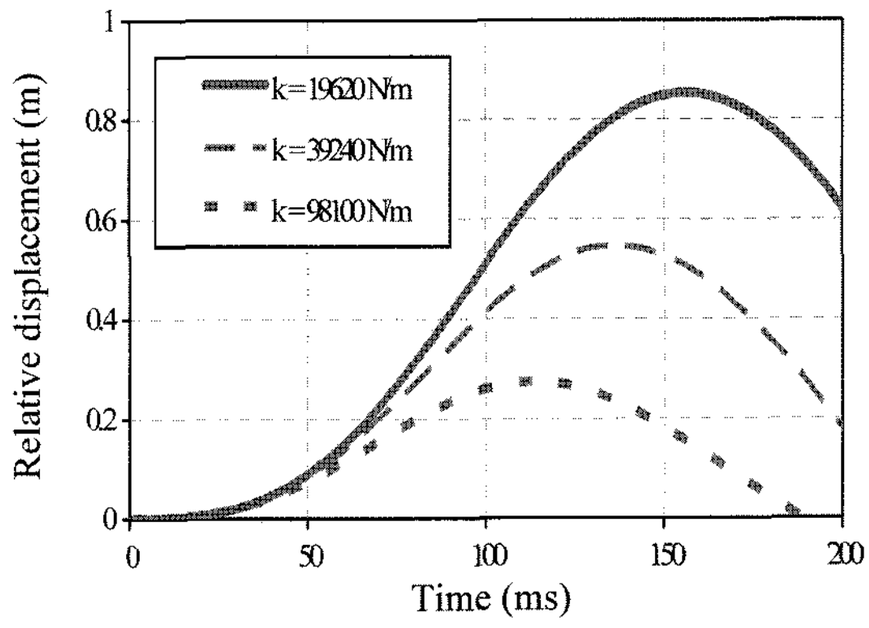

Figure 14. Relative displacement of the adult occupant in full frontal collision with different stiffness values.

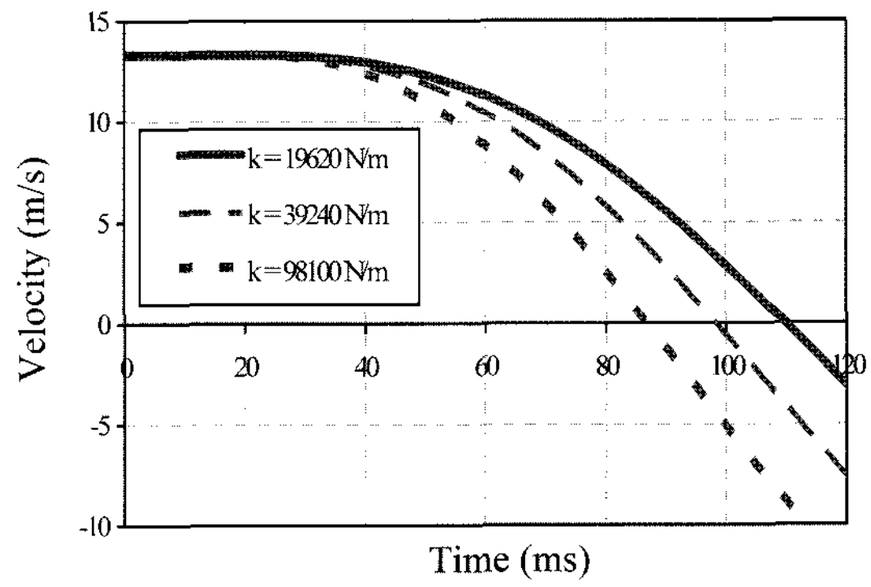

Figure 15. Velocity of the adult occupant in full frontal collision with different stiffness values.

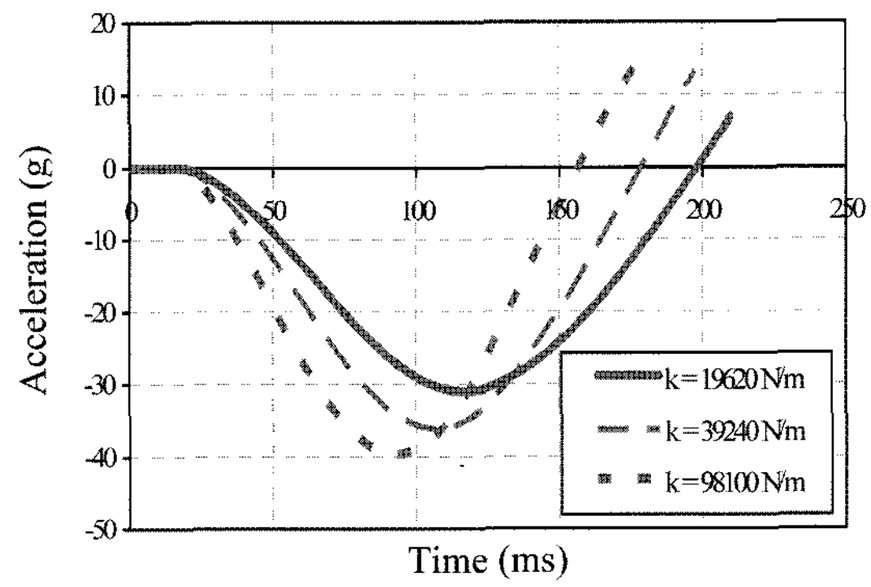

Figure 16. Acceleration of the adult occupant in full frontal collision with different stiffness values.

Figure 13. The peak acceleration is observed to be 40 g at 50% and 50 g at a value of 10% of the critical damping.

The influence of the stiffness value of the restraint system at a constant damping value of 50% of the critical damping is investigated. Three different stiffens values of the occupant's restraint system, 98.1, 39.24, and 19.62 kN/m, are considered in this paper. Figures 14, 15 and 16 show the relative displacement, velocity and acceleration of the adult occupant as obtained from the full frontal collision simulation.

It is clear from Figure 14 that a significant reduction in the displacement injury is observed with increase in the stiffness of the restraint system. It is also observed that the stiffness values of the restraint system have a

significant influence on the velocity of the occupant when it ranges from 19.62 kN/m to 98.1 kN/m as shown in Figure 15. The acceleration of the occupant decreases with decrease in the stiffness values. This can be concluded by noting that the acceleration decreases from 40 g at a higher stiffness value to 30 g at the lower value of the stiffness as shown in Figure 16. It is worthy to note that the acceleration pulse in the case of higher stiffness values is shorter than that caused by a softer restraint system.

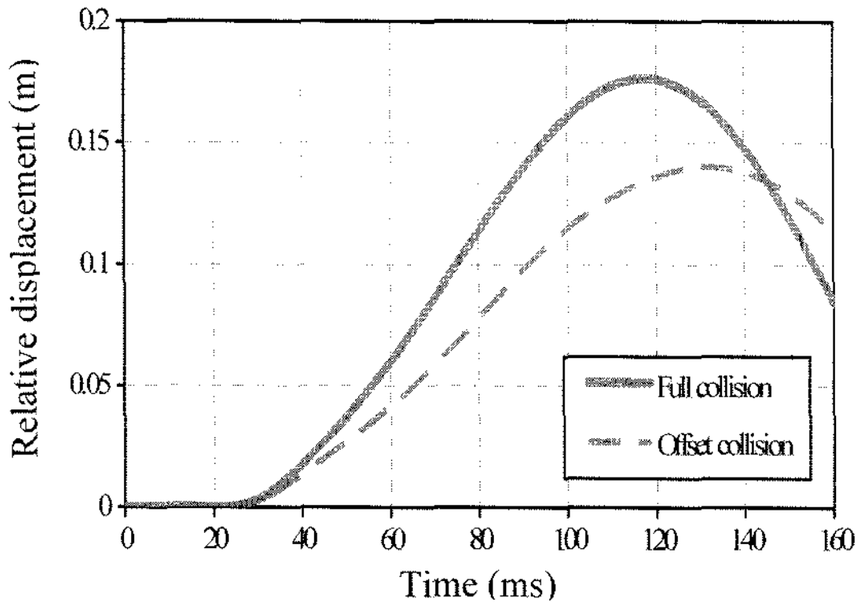

Figure 17. Relative displacement of the child occupant in full and offset frontal collisions.

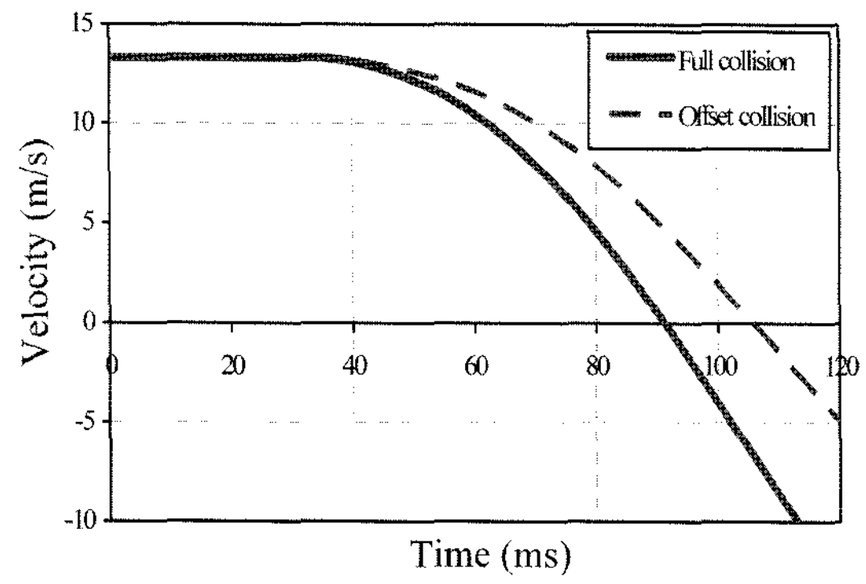

Figure 18. Velocity of the child occupant in full and offset frontal collisions.

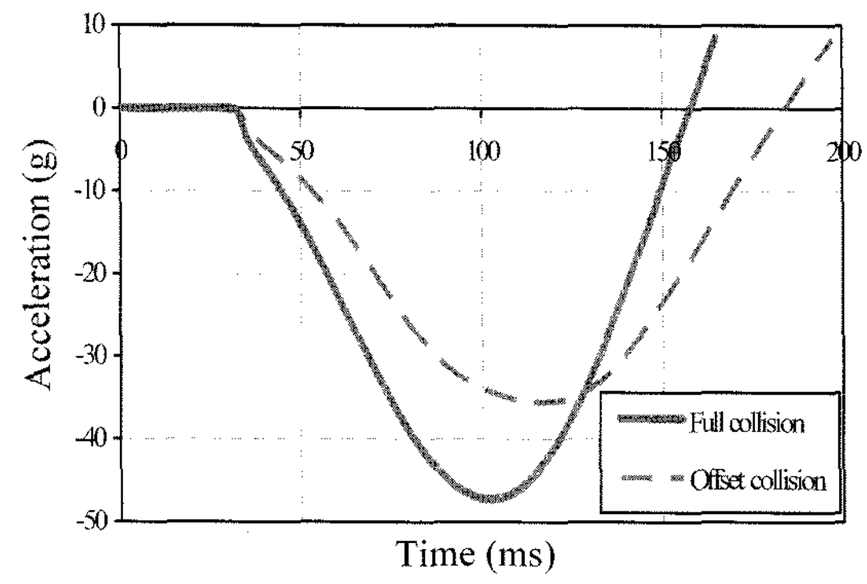

Figure 19. Acceleration of the child occupant in full and offset frontal collisions.

4.2. Child Occupant

Two cases of crash simulation, full and offset events, runs involving two vehicles in head-on collision are studied with child occupant. The first case involved a collision of two vehicles in a full frontal collision. The second case involved the two vehicles in an offset frontal collision. The time histories of the relative displacement, velocity and acceleration of the child occupant as obtained from the two simulations are depicted in Figures 17, 18 and 19, respectively.

Figure 17 clearly shows the significant reduction in the displacement injury in the case of offset frontal collision. This can be concluded by noting that the occupant relatively displaced 0.14 m in the offset collision compared to 0.18 m in the full frontal collision. It is clear from Figure 18 that the child occupant's velocity vanishes in a longer time zone in the offset collision than that in the full frontal collision. This indicates the time required to stop the vehicle in offset collision is larger than required in the full collision. The child occupant's acceleration is depicted in Figure 19 for both cases. It is observed that the occupant sustains more acceleration (47 g) in the full frontal collisions compared to 36 g in case of offset collision.

5. SUMMARY AND CONCLUSIONS

In this paper, the dynamic response of both adult and child occupants are studied and predicted. Two vehicles in head-on collision are used to creat the sudden impulse load on the occupant in both full and offset collision scenarios.

A simple mathematical model methodology is proposed as an effective way to predict the occupant dynamic response. Furthermore, the equations of motion of the occupants during vehicle collisions are developed and numerically solved. The occupant's acceleration and relative displacement are used as injury criteria to interpret the results. It is demonstrated from the numerical simulations that the dynamic response and injury criteria are easily captured and analyzed. In addition, it is shown that the stiffness and damping values of the restraint system significantly influence the dynamic response of both child and adult occupants. It is also shown that the mathematical models can be effectively used for a rapid analysis before costly and time consuming large scale finite element analysis is performed.

REFERENCES

Bennette, J., Lust, R., and Wang, J. (1991). Optimal design strategies in crashworthiness and occupant protection. *The ASME Mechanical Engineering Congress and*

Exposition, New York, USA, 51–66.
Canadian Motor Vehicle Safety Standards (CMVSS) (1999). *Child Restraint Systems.* Standard No. 213.
Elmarakbi, A. (2004). *Dynamic Modeling and Analysis of Vehicle's Smart Front-End Structure for Frontal Collision Improvement.* Ph. D. Dissertation. University of Toronto. Toronto. Canada.
Elmarakbi, A. and Zu, J. (2004). Dynamic modeling and analysis of smart vehicle structures for frontal collision improvement. *Int. J. Automotive Technology* **5**, **4**, 247–255.
Elmarakbi, A. and Zu, J. (2005). Crashworthiness improvemenet of vehicle-to-rigid fixed barrier in full frontal impact using novel vehicle's front-end structures. *Int. J. Automotive Technology* **6, 5**, 491–499.
Federal Motor Vehicle Safety Standards (FMVSS) (1999). *Occupant Crash Protection.* Title 49, 5, Standard No. 208.
Federal Motor Vehicle Safety Standards (FMVSS) (1999). *Child Restraint Systems.* Title 49, 5, Standard No. 213.
Hyde, A. (1992). Crash Injuries: How and why they happen. 6–27.
Kamal, M. (1970) Analysis and simulation of vehicle-to-barrier impact. *SAE Paper No.* 700414.
Mills, P. and Hobbs, C. (1984). The probability of injury to car occupants in frontal and inside impacts. *SAE Paper No.* 841652.